Near-Infrared-Emitting Nanoparticles for Lifetime-Based Multiplexed Analysis and Imaging of Living Cells

Katrin Hoffmann,[†] Thomas Behnke,[†] Daniela Drescher,[†,‡] Janina Kneipp,[†,‡] and Ute Resch-Genger[†,*]

[†]BAM Federal Institute for Materials Research and Testing, Richard-Willstaetter-Straße 11, 12489 Berlin, Germany, and [‡]Department of Chemistry, Humboldt-Universität zu Berlin, Brook-Taylor-Straße 2, 12489 Berlin, Germany

ABSTRACT The increase in information content from bioassays and bioimaging requires robust and efficient strategies for the detection of multiple analytes or targets in a single measurement, thereby addressing current health and security concerns. For fluorescence techniques, an attractive alternative to commonly performed spectral or color multiplexing presents lifetime multiplexing and the discrimination between different fluorophores based on their fluorescence decay kinetics. This strategy relies on fluorescent labels with sufficiently different lifetimes that are excitable at the same wavelength and detectable within the same spectral window. Here, we report on lifetime multiplexing and discrimination with a set of nanometer-sized particles loaded with near-infrared emissive organic fluorophores chosen to display very similar absorption and emission spectra, yet different fluorescence decay kinetics in suspension. Furthermore, as a first proof-of-concept, we describe bioimaging studies with 3T3 fibroblasts and J774 macrophages, incubated with mixtures of these reporters employing fluorescence lifetime imaging microscopy. These proof-of-concept measurements underline the potential of fluorescent nanoparticle reporters in fluorescence lifetime multiplexing, barcoding, and imaging for cellular studies, cell-based assays, and molecular imaging.

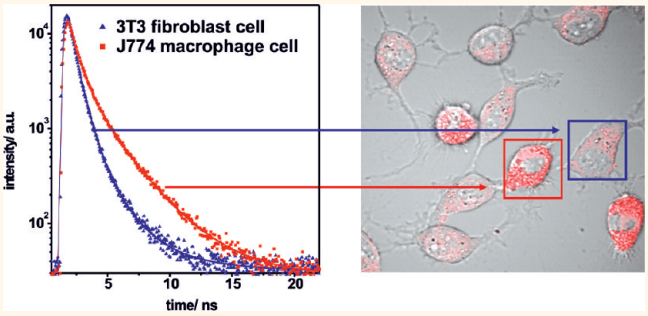

KEYWORDS: fluorescence lifetime imaging microscopy · FLIM · lifetime multiplexing · near-infrared · NIR · cell imaging · nanoparticles

Fluorescence techniques are among the most frequently employed methods in bioanalysis and biomedical imaging due to their comparable ease of use, high sensitivity, and high information content providing several analyte-specific quantities simultaneously,[1] even in complex biological systems.[2] At the core of all fluorescence-based methods are fluorescent labels or reporters, acting, for example, as signaling units in targeted probes or sensor molecules, which can be excited and detected with common commercial instruments.[3−8] Important features of suitable fluorophores are a high brightness, excellent long-term stability, negligible toxicity, and minimum nonspecific interactions with, for example, a complex biomatrix. In addition, there is an increasing interest in fluorophores that enable the simultaneous detection of several analytes or targets in multiplexed assays or in sensing and imaging applications. Typically, the increase in information content from bioassays and bioimaging is achieved with spectral multiplexing exploiting dyes that can be excited at the same wavelength and distinguished by their different emission spectra. Alternatively, donor−acceptor dye combinations can be used. This, however, requires either different detectors, one for each emission color, or a spectrally resolving detection system.[9] Despite the ever-increasing variety of commercial organic fluorophores, spectral multiplexing with organic dyes is hampered by the comparatively broad, often overlapping absorption and emission spectra and the typically small Stokes shifts, favoring spectral crosstalk in emission.[3] An attractive option presents fluorescence lifetime multiplexing, *i.e.*, the discrimination between fluorophores based on their different fluorescence decay kinetics. This approach relies on fluorescent labels with sufficiently different lifetimes, yet excitable at the same wavelength and detectable

* Address correspondence to Ute.resch@bam.de.

Received for review March 4, 2013 and accepted July 2, 2013.

Published online July 09, 2013
10.1021/nn4029458

within the same spectral window. Moreover, in contrast to relative fluorescence intensities, the fluorescence lifetime is insensitive to variations in excitation light intensity and dye concentration. This renders fluorescence lifetime measurements ideal for imaging and sensing applications[10,11] and multiplexed detection and barcoding.[12] For cellular and also *in vivo* imaging studies, fluorescence measurements in the near-infrared (NIR) are favorable to minimize unspecific background signals and increase the penetration depth of the excitation light.[10,11,13] The vast majority of the few lifetime multiplexing applications reported, however, have been performed with fluorophores emitting in the visible (vis) region due to restrictions imposed by the photophysics of organic dyes.[1] Up to now, there are only very few studies on imaging and lifetime multiplexing with NIR-emissive dyes,[14−18] due to the often reported sensitivity of their spectroscopic properties to their local environment and limited signal intensity, stability, and water solubility. Dye encapsulation elegantly circumvents possible interactions with their surrounding matrix.[19,20] This can be advantageous, for example, for the design of fluorescent reporters for lifetime-based fluorescence imaging of cells since this strategy should render the decay kinetics of each particle independent of its location within the cell and enable the prediction of label decay kinetics from time-resolved fluorescence measurements with the reporters in suspension. Moreover, dye-loaded polystyrene (PS) nanoparticles (PSNP) also permit the use of hydrophobic dyes[21−23] and the development of ratiometric probes[24] and improve label brightness.[1,25−34] In addition, the incorporation of NIR fluorophores into NPs often enhances their photostability and minimizes their possible chemical and photochemical cytotoxicity.[35−39]

This encouraged us to study different organic dyes encapsulated in PSNP for the development of a platform of fluorescent reporters for lifetime multiplexing and imaging, *e.g.*, to enable the detection and monitoring of different targets and interactions between probe and biomolecules,[40] and to perform fluorescence lifetime imaging studies in the NIR. PSNP were chosen here because of their negligible toxicity in cellular and animal studies[21,24] and their availability with different surface groups, enabling straightforward functionalization with, for example, biomarker-specific ligands such as antibodies.[21] Although this encapsulation approach was expected to yield complex decay kinetics due to the heterogeneity of the dye microenvironment in the PS matrix, previous studies with mixtures of quantum dots and organic dyes, all revealing multiexponential decay kinetics, demonstrated that even under such conditions label discrimination and quantification are possible.[16,41−45]

Here, we report on a newly prepared set of differently sized PSNP loaded with NIR dyes absorbing and emitting in the same spectral window, yet revealing different fluorescence decay kinetics, and their application in a proof-of-principle study on lifetime multiplexing in living cells. In this respect, we studied the potential of fluorescence lifetime-based analysis to distinguish between differently stained PSNP in suspension as well as in fibroblast and macrophage cells incubated with different mixtures of these particles employing fluorescence lifetime imaging microscopy (FLIM).

RESULTS AND DISCUSSION

Spectroscopic Properties of Encapsulated NIR Fluorescent Dyes. For the preparation of 25 nm- and 100 nm-sized PSNP, we used a previously described staining procedure that does not affect the size or the size distribution of the originally monodisperse particles.[22,23,46] Several hydrophobic NIR dyes were evaluated in organic solvents. Criteria for dye choice included the feasibility for (i) excitation at the same wavelength (determined by the spectral position of the absorption band), (ii) detection at the same emission wavelength/emission channel (controlled by the spectral position of the emission band), and (iii) sufficiently different fluorescence lifetimes, preferably varying by a factor of at least two. Especially the latter requirement presents a considerable challenge for NIR emitters, which commonly reveal relatively short fluorescence lifetimes in the range of *ca.* 0.5 to 2.0 ns, with very few exceptions such as certain squaraine dyes[47] and pyrrolopyrrole cyanines.[48] On the basis of these requirements, we chose the asymmetric cyanine Itrybe[23] and the commercially available squaraine dye Sq730 for this study. The broad and unstructured absorption and emission spectra of Itrybe and its relatively large Stokes shift (Figure 1) suggest a considerable charge transfer character of the underlying optical transitions.[1] Sq730 shows relatively narrow and slightly structured absorption and emission bands in organic solutions, characteristic of a dye with optical transitions delocalized over the whole chromophore (Figure 1). The emission spectra of both dyes encapsulated in the apolar and rigid PS matrix closely resemble the spectral shape and position of the corresponding spectra in tetrahydrofuran (THF). Due to signal-distorting scattering effects, the absorption spectra of the dye-loaded PSNP were omitted in Figure 1.[46] The negligible influence of the PS matrix on the spectroscopic properties is a particularly beneficial property of both dyes. It allows measurements of the free dyes in solution and of the stained particles using identical excitation and emission parameters, *e.g.*, in fluorescence spectroscopy and microscopy.

Screening studies to assess the principal potential of these dye-loaded PSNP revealed that they are photostable for weeks in water and do not show any signs of dye leaking.[23] They display high fluorescence

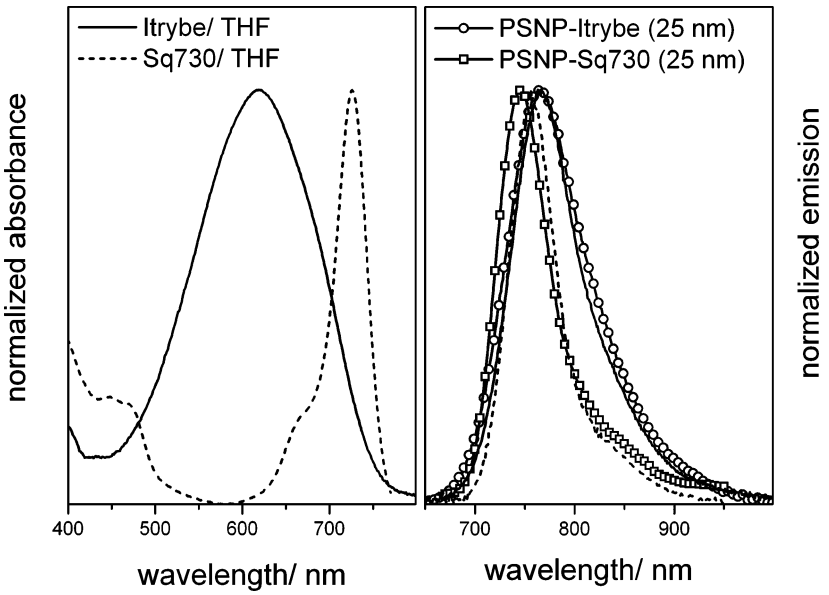

Figure 1. Absorption and corrected emission spectra of Itrybe (solid lines) and Sq730 (dotted lines) in THF and their emission spectra encapsulated in PSNP in water (PSNP-Itrybe —○—; PSNP-Sq730 —□—).

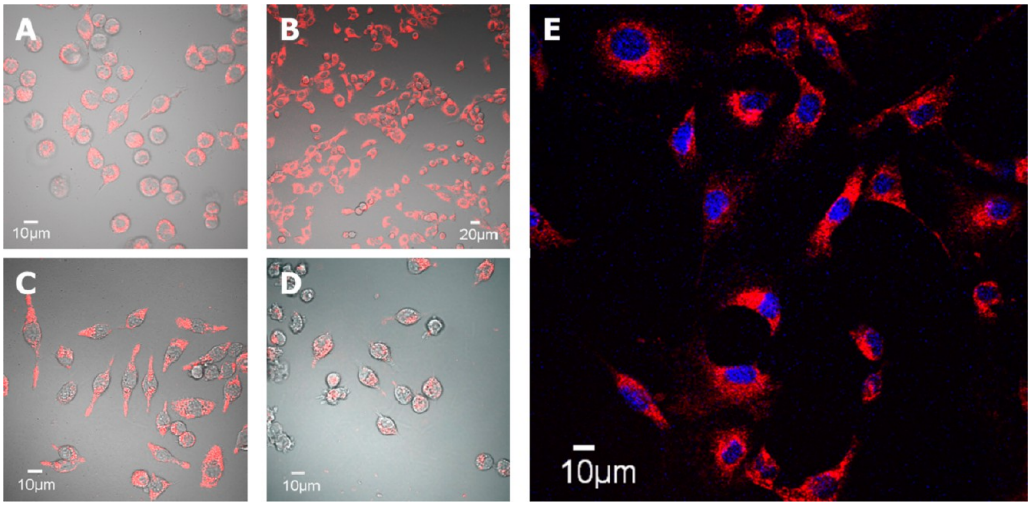

Figure 2. Fluorescence micrographs of J774 macrophages (A) and 3T3 fibroblast cells (B, E), incubated with 25 nm-sized PSNP-Itrybe. Excitation was at 633 nm, and the emission was detected in the wavelength region between 685 and 760 nm. Panel E additionally illustrates the positions of the DAPI-stained cell nuclei (excitation at 351 nm; emission channel 400−475 nm). The bottom panels show the emission between 685 and 760 nm of J774 macrophages exposed to 100 nm-sized PSNP-Itrybe (C) and 100 nm-sized PSNP-Sq730 (D) upon excitation at 633 nm (microscope objective UPLSAPO 60×O/1.35).

intensities in aqueous suspension and keep these properties also after uptake by living cells.[49] In Figure 2, fluorescence micrographs of J774 macrophage cells (2A) and 3T3 mouse fibroblast cells (2B, 2E), incubated with 25 nm-sized PSNP-Itrybe are shown. The right panel (2E) indicates the positions of the cell nuclei that were additionally stained with DAPI. The fluorescence images of J774 macrophages exposed to 100 nm-sized PSNP-Itrybe and 100 nm-sized PSNP-Sq730 are displayed in the bottom panels 2C and 2D, respectively. These results underline the general advantage of our encapsulation strategy to turn hydrophobic NIR fluorophores into stable and bright labels for biological applications in aqueous media.

Fluorescence Lifetime Measurements. Itrybe and Sq730 display a high degree of spectral overlap in emission (Figure 1), rendering their discrimination in the intensity domain very difficult.[50] The fluorescence lifetimes τ_f of the free dyes Sq730 and Itrybe in THF with $\tau_f = 2.94 \pm 0.02$ ns and $\tau_f = 0.94 \pm 0.01$ ns, respectively, are, however, sufficiently different. Both lifetimes obtained from monoexponential fits of the measured decay curves differ by a factor of about three. Hence, fluorescence measurements in the time domain can enable the discrimination between these NIR-emissive dyes. A prerequisite for simultaneous lifetime-based multiplexed analysis of two or more fluorophores is the proper characterization of the fluorescence decays of

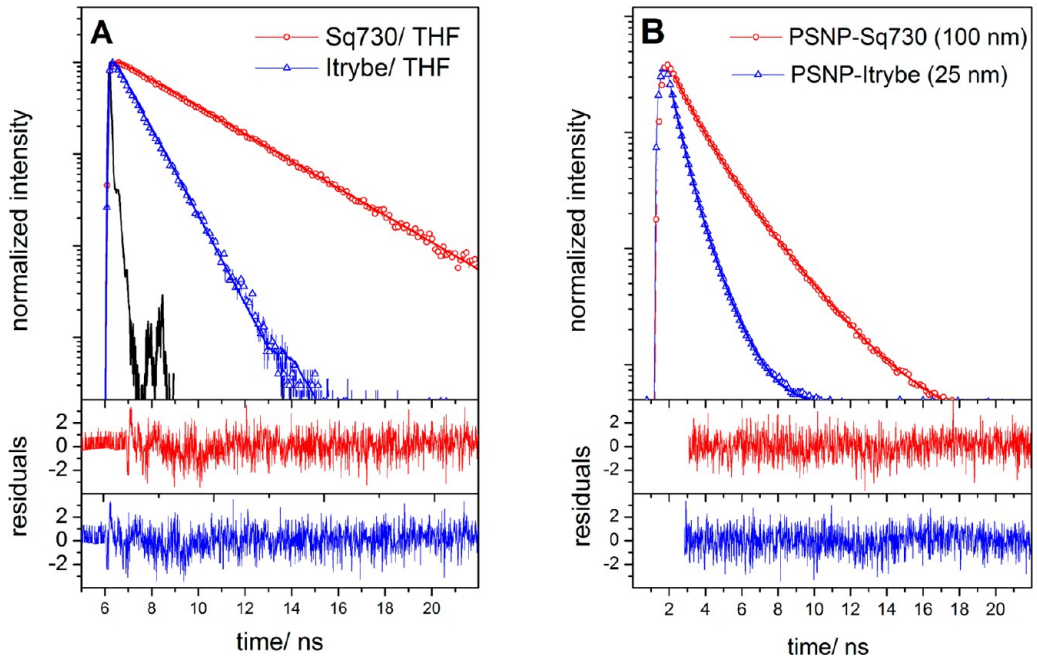

Figure 3. (A) Measured and monoexponentially fitted fluorescence decay curves of Itrybe and Sq730 in THF measured with the lifetime spectrometer FLS 920. (B) PSNP-Itrybe (25 nm, −△−) and PSNP-Sq730 (100 nm; −○−) decays in water suspensions collected and biexponentially fitted using the FLIM microscope. The lower panels represent the corresponding residuals characterized by small fluctuations. Details on the performance and data evaluation of the time-resolved fluorescence measurement are given in the Materials and Methods section.

the individual reporters. Aiming at the evaluation of the potential of NIR-emitting particle labels, the dyes Itrybe and Sq730 were studied in PSNP. Time-resolved fluorescence measurements in aqueous suspension demonstrated also for these encapsulated dyes a clearly distinguishable fluorescence decay behavior, although the heterogeneous dye microenvironment in the PS matrix renders the decay kinetics more complex. The monoexponential fluorescence decays of the free dyes Sq730 and Itrybe in THF and the corresponding lifetime data obtained for aqueous suspensions of PSNP loaded with these dyes are shown exemplarily in Figure 3A and B. Despite their different decay kinetics, the fluorescence lifetimes τ_f of the free dyes Sq730 and Itrybe in THF correspond to the biexponentially fitted average lifetimes measured in PSNP, thus suggesting only negligible sensitivity of these parameters to the environment (Table 1).

For the description of the measured decay curves of the particle reporters, at least two decay components are necessary, as shown exemplarily in Table 1 for 25 nm-sized PSNP-Itrybe and 100 nm-sized PSNP-Sq730, respectively. For encapsulated Sq730, biexponential decay kinetics with fluorescence lifetimes of $\tau_1 \sim 3.4$ ns (normalized relative amplitude $A_1 \sim 0.64$) and $\tau_2 \sim 1.6$ ns (normalized relative amplitude $A_2 \sim 0.35$) were observed. This yields an amplitude-weighted fluorescence lifetime $\tau_{Amp} \sim 2.8$ ns and an intensity-weighted lifetime $\tau_{Int} \sim 3.0$ ns. The biexponential fitting procedure applied to the fluorescence decays of Itrybe-loaded PSNP results in $\tau_2 \sim 1.3$ ns (normalized relative amplitude $A_1 \sim 0.36$) and $\tau_3 \sim 0.6$ ns (normalized relative amplitude $A_2 \sim 0.64$), yielding mean lifetimes of $\tau_{Amp} \sim 0.9$ ns and $\tau_{Int} \sim 1.0$ ns, respectively. Both types of lifetimes τ_{Amp} and τ_{Int}, which are used equally in the literature, differ in the way the individual decay times of the fluorophores in the mixture are weighted in the fitting routine. The average lifetimes[51,52] were obtained from the integral emission intensity $\tau_{Int} = \sum_j Amp_j\tau_j^2/\sum_j Amp_j\tau_j$ (intensity-weighted) or from the initial fluorescence intensity at $t = 0$ $\tau_{Amp} = \sum_j Amp_j\tau_j/\sum_j Amp_j$ (amplitude-weighted), respectively.

Fluorescence Lifetime Imaging Microscopy of Living Cells. To evaluate the suitability of the NIR-emissive particles as reporters for lifetime multiplexing and barcoding in cells, we incubated 3T3 fibroblast and J774 macrophage cells with mixtures of PSNP loaded with Itrybe and Sq730. Dynamic light scattering measurements confirm the absence of particle agglomeration in the incubation media for all particle sizes and concentrations used (data not shown). Different particle sizes provide a simple means to control reporter uptake and reporter localization, thereby omitting the need for a surface functionalization of the particles with targeting ligands in the design of these cell experiments. While fibroblast cells are very well suited to study endocytosis of smaller nanoparticles (below 100 nm in diameter), macrophage cells are capable of an efficient internalization of both small and larger particles with sizes up to 3 μm.[53−56] Thereby, they serve as a positive control, taking up all types of particles with comparable efficiency. Previously performed, detailed studies revealed

TABLE 1. Fluorescence Lifetime Parameters Extracted from FLIM Measurements with PSNP-Itrybe (25 nm) and PSNP-Sq730 (100 nm) Suspended in Water and from FLIM Images of J774 Macrophage Cells and 3T3 Fibroblast Cells Incubated with These Particles[a]

	PSNP-Itrybe			PSNP-Sq730			PSNP-Itrybe/PSNP-Sq730	
parameter	water[b]	3T3 cells	J774 cells	water[c]	3T3 cells	J774 cells	3T3 cells	J774 cells
τ_1/ns				3.39 ± 0.05	3.29 ± 0.04	2.94 ± 0.07	3.26 ± 0.21	3.31 ± 0.22
A_1				0.64 ± 0.04	0.66 ± 0.06	0.46 ± 0.07	0.09 ± 0.02	0.17 ± 0.07
τ_2/ns	1.34 ± 0.01	1.02 ± 0.04	1.42 ± 0.09	1.58 ± 0.06	1.47 ± 0.01	1.08 ± 0.11	1.37 ± 0.25	1.61 ± 0.12
A_2	0.36 ± 0.05	0.37 ± 0.04	0.22 ± 0.06	0.35 ± 0.05	0.34 ± 0.02	0.54 ± 0.07	0.34 ± 0.08	0.37 ± 0.05
τ_3/ns	0.62 ± 0.01	0.52 ± 0.03	0.67 ± 0.03				0.59 ± 0.05	0.62 ± 0.03
A_3	0.64 ± 0.05	0.63 ± 0.06	0.78 ± 0.05				0.57 ± 0.10	0.46 ± 0.10
τ_{Amp}/ns	0.88 ± 0.05	0.72 ± 0.04	0.83 ± 0.06	2.75 ± 0.03	2.68 ± 0.04	2.11 ± 0.31	1.09 ± 0.09	1.45 ± 0.15
τ_{Int}/ns	0.99 ± 0.07	0.80 ± 0.05	0.95 ± 0.08	3.02 ± 0.01	2.95 ± 0.02	2.37 ± 0.16	1.64 ± 0.13	2.07 ± 0.14
χ^2	1.07 ± 0.03	1.08 ± 0.02	2.51 ± 1.23	1.08 ± 0.05	1.02 ± 0.02	4.84 ± 2.68	1.02 ± 0.06	1.03 ± 0.10

[a] The lifetimes are derived from biexponentially fitted decay curves. The measured decay curves from particle mixtures of PSNP-Itrybe/PSNP-Sq730 of 1:1 in a co-culture experiment (3T3 cells/J774 cells of 5:1) were fitted with a three-exponential decay function, resulting in amplitude-weighted and intensity-weighted average lifetimes τ_{Amp} and τ_{Int}, respectively. τ_i are the lifetimes of each component i, and A_i the corresponding fractional amplitudes. [b] Itrybe in THF: $\tau_f = 0.94 \pm 0.01$ ns (cuvette measurement). [c] Sq730 in THF: $\tau_f = 2.94 \pm 0.02$ ns (cuvette measurement).

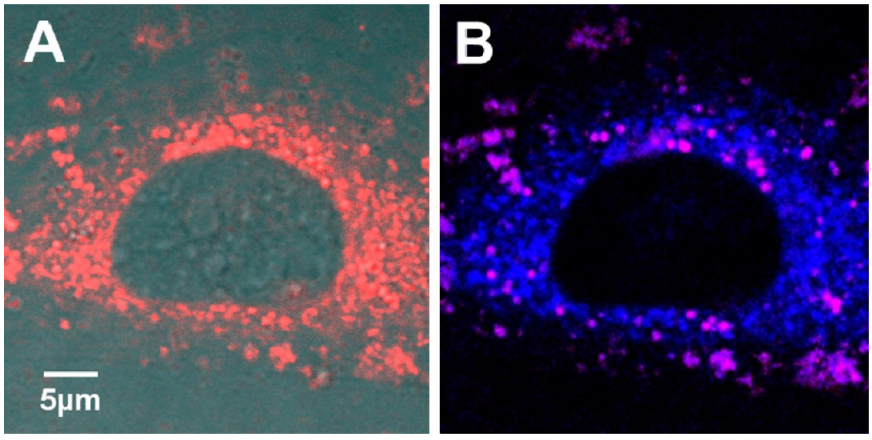

Figure 4. Confocal laser scanning microscopy (CLSM) image (A) and lifetime-based FLIM image (B) of a living 3T3 cell, incubated with a 2:1 mixture of PSNP-Itrybe (25 nm) and PSNP-Sq730 (100 nm). The microscopy image (A) shows an overlay of the transmission channel with the fluorescence channel using a detection window between 685 and 785 nm (excitation at 633 nm). The FLIM image (B) was calculated from three fixed fluorescence lifetimes (excitation at 640 nm; detection range determined by an emission filter 685/70 nm). For clarity of visualization, the third lifetime related to both particle reporters (see Table 1) is not displayed. The color code is chosen to depict the amplitude of the short-lived component mostly originating from PSNP-Itrybe in blue and the amplitude of the long-lived component related to Sq730 in red, respectively.

no influence of cell treatment with dye-loaded PSNP on cell viability[21,57] in the concentration range applied in our experiments. In accordance with the assumption that in our experiments viability is not affected by the presence of the nanoparticles, both macrophage and fibroblast cells maintained their native morphology during and after particle incubation.

The results of the steady-state and time-resolved fluorescence imaging experiments on PSNP within cells are highlighted in Figure 4 exemplarily for a 3T3 cell incubated with two different, lifetime-encoded particle types. For these studies, the fibroblast cells were exposed to a mixture of 0.1 wt % of 25 nm-sized PSNP-Itrybe and 100 nm-sized PSNP-Sq730 in a mass ratio of 2:1 for one hour. As expected from their emission spectra (Figure 1), these two types of particles cannot be distinguished by integral measurements of fluorescence intensity, as follows from the fluorescence microscopy image in Figure 4A, showing both dye-loaded PSNP in the same detection window between 685 and 785 nm. Fluorescence measurements in the time domain, however, enable the discrimination between these spectrally similar labels (Figure 4B), which will be described and discussed in detail below. The fluorescence decay behavior of the particle reporters in the cells is comparable to that observed for the encapsulated dyes in aqueous suspension. This is an important prerequisite for lifetime-based analysis of such systems as well as for cellular and molecular imaging studies.[50,58] For the intended multiplexing and barcoding applications, this insensitivity to the surrounding environment renders dye-loaded particle

labels superior to molecular fluorescent reporters, whose decay kinetics are typically affected by dye microenvironment.[50,58,59]

For the FLIM experiments, series of fibroblast cells were simultaneously incubated with varying mass ratios of both types of dye-loaded PSNP at a total particle concentration of 1 mg/mL (0.1 wt %). Then, the lifetime traces upon excitation at 640 nm of individual cells incubated with these specified particle mixtures were recorded in the detection range of a 685/70 nm filter. Although the fluorescence decay kinetics of the dye-loaded PSNP are sufficiently different for the simultaneous analysis of both types of fluorescent reporters, their multiexponential decay behavior complicates the evaluation of the lifetime measurements as compared to species with ideal monoexponential decay kinetics. Mixtures of both types of particles, each displaying biexponential decays, result in theory in four decay terms. However, as both types of fluorescent reporters reveal a decay component with a similar lifetime between 1.3 and 1.6 ns (amplitude A_2 in Table 1) in water, we could adequately describe the decay curves of particle mixtures measured within cells already with a three-term exponential decay function (see Supporting Information Table S2 and Figure S1). In the case of a 1:1 mixture of PSNP-Itrybe and PSNP-Sq730, three decay times, *i.e.*, ~3.5, ~1.7, and ~0.7 ns, with relative amplitudes of ~0.28, ~0.37, and ~0.35, respectively, were required to fit the measured decay curves. The fitting procedure yielded average lifetimes of $\tau_{Amp} \sim 1.8$ ns and $\tau_{Int} \sim 2.5$ ns.

On the basis of these fits, the FLIM image of the fibroblast cell exposed to a mixture of 25 nm-sized PSNP-Itrybe and 100 nm-sized PSNP-Sq730 was calculated pixel-by-pixel (see, for example, Figure 4B). Here, the lifetimes of the long-lived component (~3.5 ns), characteristic of PSNP-Sq730, and the short-lived decay (~0.7 ns), typical of PSNP loaded with Itrybe, were used for reporter discrimination. The lifetime of the second decay component, assigned to both particle systems (Table 1 above), was neglected in the FLIM image in order to simplify the assessment of the fluorescence lifetimes of the cell. As illustrated in Figure 4B, the amplitudes of the short lifetimes (blue), which are associated with 25 nm-sized PSNP-Itrybe, are homogeneously distributed all over the cytoplasm of the fibroblast cell. In contrast, the amplitudes of the long lifetimes (red), characteristic of 100 nm-sized PSNP-Sq730, can be observed in distinct areas of the cytoplasm and at the cell surface. No particles were found inside the cell nucleus (see also Figure 2E). These findings suggest that for the applied incubation conditions 25 nm-sized PSNP-Itrybe may be taken up and processed differently compared to 100 nm-sized PSNP-Sq730. Since nanoparticle uptake by fibroblast cells occurs mostly by endocytosis, both dye-loaded PSNP species are localized in endosomal vesicles. As visible in Figure 4B, the distribution of the vesicles containing 25 nm- and 100 nm-sized PSNP inside the cell differs. In addition to their distinct locations, endosomes in the fibroblast cells resulting from uptake of nanoparticles of different sizes are also expected to vary in number and sizes, which can be explained by differences in the uptake mechanism.[57,60] The images of the cells provide evidence that this may also be the case in our experiments with 25 nm- and 100 nm-sized PSNP. To investigate a possible influence of cell type, that is, uptake and processing behavior on reporter fluorescence decay, experiments were also performed with J774 macrophage cells (see Figure 2A, C, and D).[53−55] The fluorescence decay behavior of both types of reporters matched that observed in suspension and in fibroblast cells (see Table 1), and the results indicate an efficient PSNP uptake independent of particle size.

Fluorescence decay curves from FLIM studies with 3T3 and J774 cells incubated with different mixtures of dye-loaded PSNP are shown in Figure 5A and C, respectively. Fibroblast cells were incubated with 25 nm-sized PSNP-Itrybe and 100 nm-sized PSNP-Sq730 for one hour, while macrophage cells were exposed to PSNP-Itrybe and PSNP-Sq730, both with a 100 nm size. The corresponding ratio-dependent average lifetimes of the cells are presented in Figure 5B and D.

When comparing the FLIM data in Figure 6B and D resulting for cells exclusively incubated with long-lived PSNP-Sq730 (fraction of Itrybe-PSNP = 0) with the data obtained for cells incubated with mixtures of both types of reporter PSNP, a systematic decrease in the average fluorescence lifetimes was found. Since this decrease corresponds to the increase in the fraction of Itrybe-loaded PSNP with their shorter lifetimes, the experiments provide a first proof-of-concept of a lifetime-based discrimination between dye-loaded particle labels with different fluorescence lifetimes or decay behavior in living cells.

Lifetime Imaging in Cell Co-culture. In order to evaluate the feasibility of a lifetime-based discrimination of particle-labeled cells, we investigated the uptake behavior of 3T3 fibroblast and J774 macrophage cells with differently sized dye-loaded PSNP in cell co-culture. In this co-culture experiment, 25 nm-sized PSNP-Itrybe and 100 nm-sized PSNP-Sq730 were simultaneously incubated in a 1:1 mass ratio with a co-culture of 3T3 and J774 cells in a ratio of 5:1 for 1 h. Hence, both cell types compete directly for the uptake of lifetime-encoded PSNP of different sizes. The differentiation of these two cell types, *i.e.*, fibroblast cells and macrophages, was done by investigation of their very specific morphological features, specific size and shape of cytoplasmic pseudopodia, and the size of the nuclei in bright field and phase contrast microscopy. Additionally, we compared the cells used in the co-culture experiment

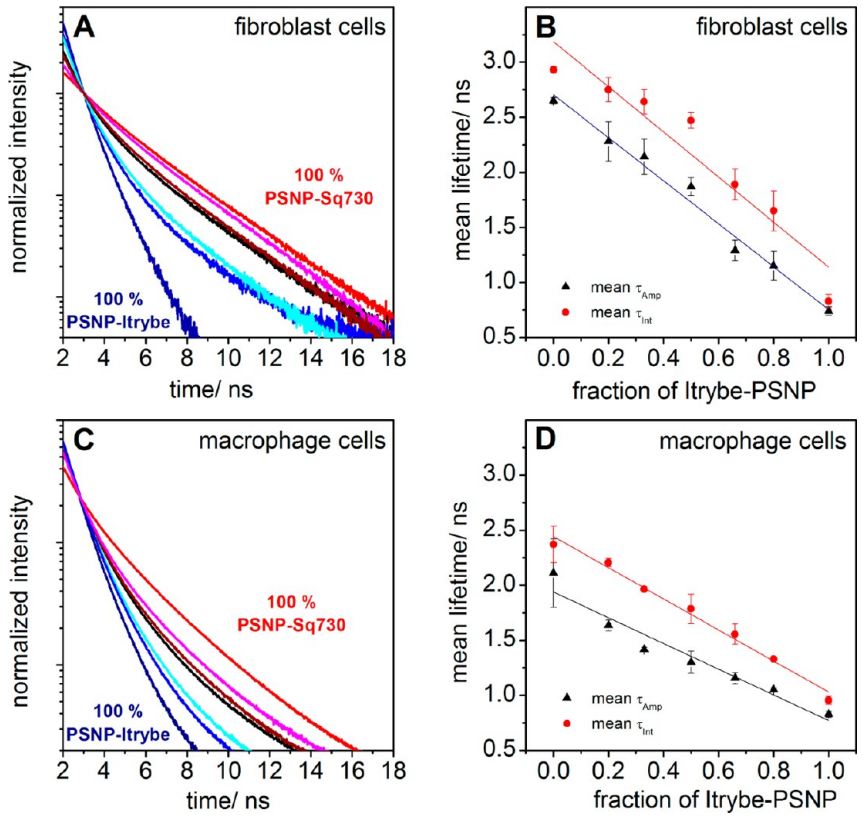

Figure 5. Fluorescence decay curves of 3T3 fibroblast cells (A) and J774 macrophage cells (C), exposed to PSNP-Itrybe (dark blue curve) and PSNP-Sq730 (red curve) and different mixtures of both components (excitation at 640 nm; detection with a detection filter of 685/70 nm). The resulting average fluorescence lifetimes τ_{Amp} (triangles) and τ_{Int} (circles) of fibroblast (B) and macrophage cells (D) were calculated from three lifetimes based on FLIM measurements.

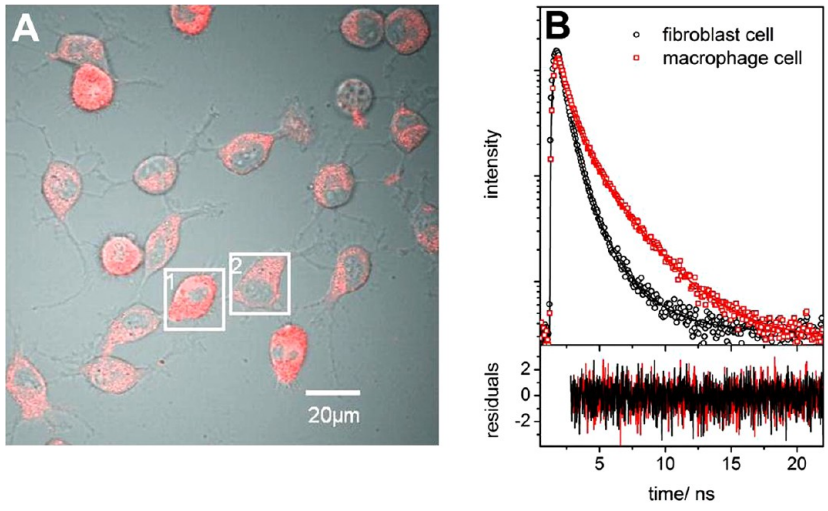

Figure 6. (A) CLSM intensity image of a macrophage cell (1) and a 3T3 fibroblast cell (2) in the co-culture studied. (B) Measured (symbols) and three-exponentially fitted (thick solid lines) fluorescence decay curves of the individual cells (macrophage: red squares, fibroblast: black circles) exposed to PSNP-Itrybe (25 nm) and PSNP-Sq730 (100 nm) in a mass ratio of 1:1. The residual traces in the bottom panel demonstrate the quality of the fits.

with those grown under identical conditions in monoculture. Detailed imaging studies of the resulting particle-labeled cells were performed with CLSM and FLIM (Figure 6).

The macrophage and the fibroblast cells, exemplarily chosen from the CLSM image of the co-culture and detected in the same spectral window (Figure 6A), cannot be spectrally distinguished. Only the resulting fluorescence intensities vary, which can be possibly ascribed to a different brightness and number of particle reporters present in the cells. The fluorescence decay curves recorded on the two cells, however,

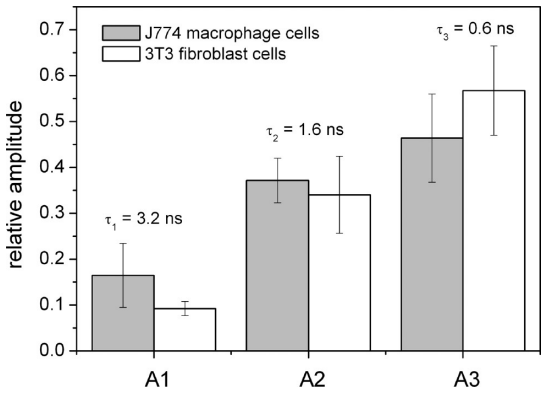

Figure 7. Relative amplitudes A_i of the lifetimes 3.2, 1.6, and 0.6 ns derived from three-exponential fits, necessary to adequately describe the measured decay curves of the J774 macrophage cells (gray) and the 3T3 fibroblast cells (white) of the co-culture experiment (number of measurements per cell type $n = 6$).

reveal significantly different decay characteristics (Figure 6B). Decay curves resulting for both cells can be satisfactorily described by three lifetimes, namely, ~3.2, ~1.6, and 0.6 ns. The χ^2 values used to evaluate the goodness of the fits and the residual traces at the bottom of Figure 6B underline the quality of this description. As follows from Figure 6B, the macrophage cell (red squares) exhibits longer decay times than the fibroblast cell (black circles), suggesting a more efficient uptake of PSNP with longer lifetimes by the macrophage. Moreover, as follows from Figure 7, the relative amplitude A_1 of the long-lived component in the macrophage exceeds the amplitude A_1 measured in the fibroblast cell, whereas the relative amplitude A_3 of the short-lived decay component (25 nm-sized PSNP-Itrybe) exhibits the opposite behavior. The long-lived component, which is associated with 100 nm-sized PSNP-Sq730, is more pronounced in the macrophage cell compared to the fibroblast. These findings support our expectation that the macrophage cell, in comparison to the fibroblast cell, probably internalizes a larger amount of the 100 nm-sized particles and that uptake efficiency for 100 nm-sized PSNP by the fibroblast cell is lower. In accordance with previous findings, our results suggest higher uptake efficiency for larger particles in the macrophage cells.[53,60,61]

If incubation of the same nanoparticle 1:1 mixture is carried out in a fibroblast monoculture (see also above), the lifetimes of these cells in a separated culture are longer than for the co-culture (cf. Supporting Information Table S2 and Table 1, respectively). This is in accordance with the expectation that, in the co-culture, the macrophage cells compete for the larger PSNP-Sq730-loaded nanoparticles. Even though the results from the co-culture and the monoculture experiment reported here are very specific for the selected nanoparticle ratio and the amount of each cell type in the co-culture, the example illustrates that the lifetime-encoded nanoparticles can be used to study uptake behavior of different cell types and mixtures.

In summary, all FLIM results obtained with our NIR-emissive PSNP in living cells demonstrate the potential of nanoparticle-based, lifetime-encoded fluorescence reporters for fluorescence lifetime imaging, lifetime multiplexing, and barcoding applications.

CONCLUSION

With Itrybe and Sq730, we identified two NIR fluorophores suitable for lifetime multiplexing in the diagnostic window using a single excitation wavelength and a single detection channel. Incorporation of these hydrophobic dyes into differently sized polystyrene nanoparticles *via* a straightforward staining procedure yielded a set of nanoscale fluorescent reporters with decay kinetics independent of particle environment, which can be surface-functionalized with a broad variety of targeting ligands. Time-resolved spectroscopic and fluorescence lifetime imaging microscopy studies with these new nanoparticle reporters enabled discrimination between probes based on their different fluorescence decay kinetics in solution, in 3T3 mouse fibroblasts, and in J774 macrophages. To the best of our knowledge, this presents the first approach of lifetime multiplexing with NIR-emissive nanometer-sized particles in living cells.

Using fluorescence lifetime imaging of living mouse fibroblast cells and macrophages incubated with mixtures of various ratios of nanoparticles differing in size and encapsulated dyes, we could demonstrate the suitability of our approach to distinguish between signals from different fractions of the two reporters based on their complex, yet characteristic decay kinetics. Using a fitting model with three decay terms for decay curves of the two dye-loaded PSPN with sufficiently different decay kinetics, we could clearly distinguish between both NIR reporters at different locations within cells. Moreover, the approach is well-suited for co-localization studies of these probes. Co-culture studies with J774 macrophages and 3T3 fibroblasts demonstrate the suitability of this concept to study the different uptake behavior of these cells and to enable the lifetime-based discrimination of different fractions of dye-doped PSNP with similar spectral properties, but different fluorescence decay kinetics by measurements of their fluorescence lifetime characteristics in a complex biological matrix.

Our results underline the potential of nanoparticle-based fluorescence lifetime multiplexing and imaging for cellular studies, cell-based assays, and molecular imaging. In the future, this strategy will be combined with spectral multiplexing to further increase the number of readout parameters. Applications will

include macrophage imaging and the development of nanoparticle-based lifetime labels and probes with different surface chemistries and recognition units for co-localization studies and multiplexed bioimaging.

MATERIALS AND METHODS

Materials. Carboxyl-functionalized polystyrene nanoparticles with diameters of 25 and 100 nm were purchased from Kisker Biotech. The dyes Itrybe (Otava Chemicals) and squaraine Sq730 (SETA Biomedicals) were encapsulated in the PSNP without further purification. The PSNP were sonicated and stained with the NIR-emitting dyes using a previously described staining procedure.[22,23,46] Tetrahydrofuran was of UV-spectroscopic grade and purchased from Sigma-Aldrich.

Cell culture media Dulbecco's modified Eagle medium (DMEM), fetal calf serum (FCS), and phosphate-buffered saline (PBS) were purchased from Biochrom AG.

Steady-State Fluorescence Spectroscopy and Microscopy. Absorption spectra were recorded on a Cary 5000 spectrometer (Varian). Fluorescence emission spectra were measured with a previously described spectrofluorometer (SLM 8100, Spectronics Instruments) in a 0°/90° measurement geometry.[62] Fluorescence microscopic images were recorded with a Fluoview 1000 (Olympus) confocal laser scanning microscope using a HeNe laser (10 mW) as excitation source (excitation wavelength of 633 nm), which was reflected by a dichroic mirror (DM 488/543/633) and focused onto the sample through an Olympus Planapochromat 60×, N.A. = 1.35 oil immersion objective. The resulting fluorescence emission was re-collected by the same objective and focused onto the photomultipliers. All fluorescence measurements were performed at room temperature.

Lifetime Measurements. Time traces of the water-insoluble dyes Itrybe and Sq730 in THF were recorded with an FLS920 fluorescence lifetime spectrometer (Edinburgh Instruments) in standard quartz cuvettes (Hellma) in a 0°/90° excitation−emission geometry using magic angle conditions (excitation polarizer set to 0° and emission polarizer set to 54.7°) with the time-correlated single-photon counting technique (TCSPC). A supercontinuum laser (Fianium SC400-2-PP) with a pulse repetition rate of 5 MHz was employed for excitation at 640 nm. The emission was detected at 740 nm (spectral bandwidth 8 nm). Deconvolution of the decay curves and fit of the fluorescence lifetimes were done with the FSP920 spectrometer software. Fluorescence lifetime imaging of cells was performed with a Fluoview 1000 (Olympus GmbH) upgraded with a FLIM-FCS upgrade kit (Picoquant GmbH) using a 640 nm laser diode (LDH-c-640, PDL800-D, pulse width <500 ps, pulse frequency or repetition rate of 40 MHz) as excitation light source and a single-channel single-photon avalanche diode as detector (emission filter 685/70 nm). Time-resolved measurements of dye-PSNP were also performed with the FLIM microscope, focused deep into droplets of the aqueous particle suspensions on a microscopy coverslip. Data acquisition and analysis were done with the TimeHarp 200 TCSPC PC-board using the software SymphoTime (Picoquant GmbH).

Data Analysis. All fits of the measured decay curves of the mixtures of dye-loaded PSNP within cells were performed with a tail-fit instead of a reconvolution procedure of the recorded decay curves with the instrument response function, which is usually mandatory for accurate analysis of fluorescence lifetimes from time-correlated single-photon counting measurements.[63] All fit parameters, the individual decay times τ_i, and the amplitudes A_i were left as freely adjustable parameters. Selected results fitted with two- or three-exponential terms either by reconvolution or by a tail-fitting procedure within the same time window (channel 130 to 1550 with 0.016 ns channel^{-1}) are summarized in Table S1 (Supporting Information). From these preliminary studies performed to optimize the fitting procedure of particle mixtures within cells the coefficient of variation of τ_{Amp} and τ_{Int} was determined to be *ca.* 10%. For the lifetime fitting a maximum likelihood estimator[51,64] has been used to account for areas with low signal intensity. χ^2 values were used to evaluate the quality of the fits. To render data analysis of the decay curves resulting for cells incubated with a single type or mixtures of nanoparticle reporters comparable, we deliberately fitted all decay curves in the same time window with three-exponential terms, which are required for the analysis of particle mixtures, although the decay curves resulting for cells incubated with a single type of reporter could be satisfactorily fitted with two exponentials (see Table S2 in the Supporting Information). This procedure of data analysis enables the straightforward comparison of changes in the average fluorescence lifetimes τ_{Amp} and τ_{Int} of these cells, which are dependent on the incubation mixtures applied. The determination of individual lifetime data was beyond the scope of our straightforward proof-of-concept approach.

To obtain the FLIM image based on the amplitudes of three components of the decay curve, a two-step approach was chosen. In a first step, both the individual lifetimes and the amplitudes were kept as freely adjustable parameters. Subsequently, the images were calculated pixel-by-pixel with fixed individual lifetimes, averaged from repeated measurements of different (at least three) cells.

Cell Culture. Mouse fibroblast cells (cell line 3T3) and macrophage cells (cell line J774; both from German Collection of Microorganisms and Cell Cultures (DSMZ), Braunschweig, Germany) were seeded out in a sterile eight-well μ-slide (ibidi GmbH, Planegg/Martinsried, Germany) and grown in DMEM with 10% FCS for 24 h in a humidified environment at 37 °C and 5% CO_2. For fluorescence microscopy, cells were incubated for 1 h with varying mass ratios of dye-loaded particles (PSNP-Itrybe to PSNP-Sq730 of 1:0; 5:1, 2:1, 1:1; 1:2; 1:5; 0:1) in standard cell culture medium, yielding a total particle concentration of 1 mg/mL (0.1 wt %). In the case of identically sized particles the mass ratio equals the number ratio. Incubation with mixtures of 100 nm- and 25 nm-sized particles in the mass ratios stated above results in particle number ratios (100 to 25 nm) of 1:0, 1:13, 1:32, 1:64, 1:128, 1:320, and 0:1. Fibroblast cells were exposed to 25 nm-sized PSNP-Itrybe and 100 nm-sized PSNP-Sq730; macrophage cells, to PSNP-Itrybe and PSNP-Sq730, both 100 nm in diameter. For the co-culture experiment, fibroblast and macrophage cells were seeded out in a ratio of 5 to 1 in sterile culture plates and incubated with PSNP-Itrybe (25 nm) and PSNP-Sq730 (100 nm) in a mass ratio of 1 to 1 (total particle concentration in culture medium 0.1 wt %). After one hour of particle incubation, cells were washed three times with PBS buffer and immediately transferred to the microscopic setup. Cells not exposed to fluorescent PSNP served as reference in all experiments.

Conflict of Interest: The authors declare no competing financial interest.

Acknowledgment. We gratefully acknowledge financial support from the Federal Ministry of Economics and Technology (BMWI-22/06 and BMWI-13/09) and from the Federal Institute for Materials Research and Testing within the framework of "BAM Innovationsoffensive". We would like to express our gratitude to Picoquant GmbH for their support with the FLIM setup. D.D. and J.K. acknowledge funding by ERC Starting Grant MULTIBIOPHOT.

Supporting Information Available: Comparative evaluation and optimization of the procedure to fit the fluorescence decay curves and detailed data on decay kinetics of different mixtures of PSNP-Itrybe and PSNP-Sq-730 in monoculture of 3T3 cells. This information is available free of charge *via* the Internet at http://pubs.acs.org.

REFERENCES AND NOTES

1. Lakowicz, J. R. *Principles of Fluorescence Spectroscopy*, 3rd ed.; Springer Science+Business Media, LLC: New York, 2006.
2. Song, E. Q.; Hu, J.; Wen, C. Y.; Tian, Z. Q.; Yu, X.; Zhang, Z. L.; Shi, Y. B.; Pang, D. W. Fluorescent-Magnetic-Biotargeting

Multifunctional Nanobioprobes for Detecting and Isolating Multiple Types of Tumor Cells. *ACS Nano* **2011**, *5*, 761–770.
3. Resch-Genger, U.; Grabolle, M.; Cavaliere-Jaricot, S.; Nitschke, R.; Nann, T. Quantum Dots *versus* Organic Dyes as Fluorescent Labels. *Nat. Methods* **2008**, *5*, 763–775.
4. Luo, S.; Zhang, E.; Su, Y.; Cheng, T.; Shi, C. A Review of NIR Dyes in Cancer Targeting and Imaging. *Biomaterials* **2011**, *32*, 7127–7138.
5. Hotzer, B.; Medintz, I. L.; Hildebrandt, N. Fluorescence in Nanobiotechnology: Sophisticated Fluorophores for Novel Applications. *Small* **2012**, *8*, 2297–2326.
6. Haase, M.; Schafer, H. Upconverting Nanoparticles. *Angew. Chem., Int. Ed.* **2011**, *50*, 5808–5829.
7. Bunzli, J. C. G. Lanthanide Luminescence for Biomedical Analyses and Imaging. *Chem. Rev.* **2010**, *110*, 2729–2755.
8. Jaiswal, J. K.; Goldman, E. R.; Mattoussi, H.; Simon, S. M. Use of Quantum Dots for Live Cell Imaging. *Nat. Methods* **2004**, *1*, 73–78.
9. Sapsford, K. E.; Berti, L.; Medintz, I. L. Materials for Fluorescence Resonance Energy Transfer Analysis: Beyond Traditional Donor-Acceptor Combinations. *Angew. Chem., Int. Ed.* **2006**, *45*, 4562–4588.
10. Berezin, M. Y.; Achilefu, S. Fluorescence Lifetime Measurements and Biological Imaging. *Chem. Rev.* **2010**, *110*, 2641–2684.
11. Abbasi, A. Z.; Amin, F.; Niebling, T.; Friede, S.; Ochs, M.; Carregal-Romero, S.; Montenegro, J. M.; Gil, P. R.; Heimbrodt, W.; Parak, W. J. How Colloidal Nanoparticles Could Facilitate Multiplexed Measurements of Different Analytes with Analyte-Sensitive Organic Fluorophores. *ACS Nano* **2011**, *5*, 21–25.
12. Mihindukulasuriya, S. H.; Morcone, T. K.; McGown, L. B. Characterization of Acridone Dyes for Use in Four-Decay Detection in DNA Sequencing. *Electrophoresis* **2003**, *24*, 20–25.
13. Adams, K. E.; Ke, S.; Kwon, S.; Liang, F.; Fan, Z.; Lu, Y.; Hirschi, K.; Mawad, M. E.; Barry, M. A.; Sevick-Muraca, E. M. Comparison of Visible and Near-Infrared Wavelength-Excitable Fluorescent Dyes for Molecular Imaging of Cancer. *J. Biomed. Opt.* **2007**, *12*, 024017-1–024017-9.
14. Widengren, J.; Kudryavtsev, V.; Antonik, M.; Berger, S.; Gerken, M.; Seidel, C. A. M. Single-Molecule Detection and Identification of Multiple Species by Multiparameter Fluorescence Detection. *Anal. Chem.* **2006**, *78*, 2039–2050.
15. Nothdurft, R.; Sarder, P.; Bloch, S.; Culver, J.; Achilefu, S. Fluorescence Lifetime Imaging Microscopy Using Near-Infrared Contrast Agents. *J. Microsc.* **2012**, *247*, 202–207.
16. Raymond, S. B.; Boas, D. A.; Bacskai, B. J.; Kumar, A. T. N. Lifetime-Based Tomographic Multiplexing. *J. Biomed. Opt.* **2010**, *15*, 046011-1–046011-9.
17. Lieberwirth, U.; Arden-Jacob, J.; Drexhage, K. H.; Herten, D. P.; Muller, R.; Neumann, M.; Schulz, A.; Siebert, S.; Sagner, G.; Klingel, S.; *et al.* Multiplex Dye DNA Sequencing in Capillary Gel Electrophoresis by Diode Laser-Based Time-Resolved Fluorescence Detection. *Anal. Chem.* **1998**, *70*, 4771–4779.
18. Zhu, L.; Stryjewski, W.; Lassiter, S.; Soper, S. A. Fluorescence Multiplexing with Time-Resolved and Spectral Discrimination Using a Near-IR Detector. *Anal. Chem.* **2003**, *75*, 2280–2291.
19. Zhang, R.; Cherdhirankorn, T.; Graf, K.; Koynov, K.; Berger, R. Swelling of Cross-Linked Polystyrene Beads in Toluene. *Microelectron. Eng.* **2008**, *85*, 1261–1264.
20. Errede, L. A.; Hanson, S. C. Polymer Swelling 0.15. Swelling and Deswelling Studies of Polystyrene Liquid-Systems in Binary-Solutions. *J. Appl. Polym. Sci.* **1994**, *54*, 619–647.
21. Behnke, T.; Mathejczyk, J. E.; Brehm, R.; Würth, C.; Ramos-Gomes, F.; Dullin, C.; Napp, J.; Alves, F.; Resch-Genger, U. Target-Specific Nanoparticles Containing a Broad Band Emissive NIR Dye for the Sensitive Detection and Characterization of Tumor Development. *Biomaterials* **2013**, *34*, 160–170.
22. Behnke, T.; Würth, C.; Hoffmann, K.; Hubner, M.; Panne, U.; Resch-Genger, U. Encapsulation of Hydrophobic Dyes in Polystyrene Micro- and Nanoparticles *via* Swelling Procedures. *J. Fluoresc.* **2011**, *21*, 937–944.
23. Behnke, T.; Würth, C.; Laux, E. M.; Hoffmann, K.; Resch-Genger, U. Simple Strategies towards Bright Polymer Particles *via* One-Step Staining Procedures. *Dyes Pigm.* **2012**, *94*, 247–257.
24. Napp, J.; Behnke, T.; Fischer, L.; Wurth, C.; Wottawa, M.; Katschinski, D. M.; Alves, F.; Resch-Genger, U.; Schaferling, M. Targeted Luminescent Near-Infrared Polymer-Nanoprobes for *in Vivo* Imaging of Tumor Hypoxia. *Anal. Chem.* **2011**, *83*, 9039–9046.
25. Seydack, M. Nanoparticle Labels in Immunosensing Using Optical Detection Methods. *Biosens. Bioelectron.* **2005**, *20*, 2454–2469.
26. Burns, A.; Ow, H.; Wiesner, U. Fluorescent Core-Shell Silica Nanoparticles: Towards "Lab on a Particle" Architectures for Nanobiotechnology. *Chem. Soc. Rev.* **2006**, *35*, 1028–1042.
27. Chan, C. P. Y.; Bruemmel, Y.; Seydack, M.; Sin, K. K.; Wong, L. W.; Merisko-Liversidge, E.; Trau, D.; Renneberg, R. Nanocrystal Biolabel with Releasable Fluorophores for Immunoassays. *Anal. Chem.* **2004**, *76*, 3638–3645.
28. Yan, J. L.; Estevez, M. C.; Smith, J. E.; Wang, K. M.; He, X. X.; Wang, L.; Tan, W. H. Dye-Doped Nanoparticles for Bioanalysis. *Nano Today* **2007**, *2*, 44–50.
29. Clark, H. A.; Hoyer, M.; Philbert, M. A.; Kopelman, R. Optical Nanosensors for Chemical Analysis inside Single Living Cells. 1. Fabrication, Characterization, and Methods for Intracellular Delivery of PEBBLE Sensors. *Anal. Chem.* **1999**, *71*, 4831–4836.
30. Morgan, T. T.; Muddana, H. S.; Altinoglu, E. I.; Rouse, S. M.; Tabakovic, A.; Tabouillot, T.; Russin, T. J.; Shanmugavelandy, S. S.; Butler, P. J.; Eklund, P. C.; *et al.* Encapsulation of Organic Molecules in Calcium Phosphate Nanocomposite Particles for Intracellular Imaging and Drug Delivery. *Nano Lett.* **2008**, *8*, 4108–4115.
31. Wolfbeis, O. S. Materials for Fluorescence-Based Optical Chemical Sensors. *J. Mater. Chem.* **2005**, *15*, 2657–2669.
32. Pauli, J.; Vag, T.; Haag, R.; Spieles, M.; Wenzel, M.; Kaiser, W. A.; Resch-Genger, U.; Hilger, I. An *in Vitro* Characterization Study of New Near Infrared Dyes for Molecular Imaging. *Eur. J. Med. Chem.* **2009**, *44*, 3496–3503.
33. Oh, W.; Jeong, Y.; Kim, S.; Jang, J. Fluorescent Polymer Nanoparticle for Selective Sensing of Intracellular Hydrogen Peroxide. *ACS Nano* **2012**, *23*, 8516–8524.
34. Sharma, P.; Brown, S.; Walter, G.; Santra, S.; Moudqil, B. Nanoparticles for Bioimaging. *Adv. Colloid Interface Sci.* **2006**, *123−126*, 471–485.
35. Sokolov, I.; Naik, S. Novel Fluorescent Silica Nanoparticles: Towards Ultrabright Silica Nanoparticles. *Small* **2008**, *4*, 934–939.
36. Burns, A. A.; Vider, J.; Ow, H.; Herz, E.; Penate-Medina, O.; Baumgart, M.; Larson, S. M.; Wiesner, U.; Bradbury, M. Fluorescent Silica Nanoparticles with Efficient Urinary Excretion for Nanomedicine. *Nano Lett.* **2009**, *9*, 442–448.
37. Muddana, H. S.; Morgan, T. T.; Adair, J. H.; Butler, P. J. Photophysics of Cy3-Encapsulated Calcium Phosphate Nanoparticles. *Nano Lett.* **2009**, *9*, 1559–1566.
38. Saxena, V.; Sadoqi, M.; Shao, J. Enhanced Photo-Stability, Thermal-Stability and Aqueous-Stability of Indocyanine Green in Polymeric Nanoparticulate Systems. *J. Photochem. Photobiol., B* **2004**, *74*, 29–38.
39. Miletto, I.; Gilardino, A.; Zamburlin, P.; Dalmazzo, S.; Lovisolo, D.; Caputo, G.; Viscardi, G.; Martra, G. Highly Bright and Photostable Cyanine Dye-Doped Silica Nanoparticles for Optical Imaging: Photophysical Characterization and Cell Tests. *Dyes Pigm.* **2009**, *84*, 121–127.
40. Houston, J. P.; Naivar, M. A.; Freyer, J. P. Digital Analysis and Sorting of Fluorescence Lifetime by Flow Cytometry. *Cytometry Part A* **2010**, *77A*, 861–872.
41. Grabolle, M.; Kapusta, P.; Nann, T.; Shu, X.; Ziegler, J.; Resch-Genger, U. Fluorescence Lifetime Multiplexing with Nanocrystals and Organic Labels. *Anal. Chem.* **2009**, *81*, 7807–7813.
42. Giraud, G.; Schulze, H.; Bachmann, T. T.; Campbell, C. J.; Mount, A. R.; Ghazal, P.; Khondoker, M. R.; Ross, A. J.; Ember,

S. W. J.; Ciani, I.; *et al*. Fluorescence Lifetime Imaging of Quantum Dot Labeled DNA Microarrays. *Int. J. Mol. Sci.* **2009**, *10*, 1930–1941.
43. Battersby, B. J.; Trau, M. Optically Encoded Particles and their Applications in Multiplexed Biomedical Assays. *Aust. J. Chem.* **2007**, *60*, 343–353.
44. Ehlert, O.; Thomann, R.; Darbandi, M.; Nann, T.; Four-Color, A. Colloidal Multiplexing Nanoparticle System. *ACS Nano* **2008**, *2*, 120–124.
45. Wilson, R.; Spiller, D. G.; Prior, I. A.; Veltkamp, K. J.; Hutchinson, A. A Simple Method for Preparing Spectrally Encoded Magnetic Beads for Multiplexed Detection. *ACS Nano* **2007**, *1*, 487–493.
46. Laux, E. M.; Behnke, T.; Hoffmann, K.; Resch-Genger, U. Keeping Particles Brilliant - Simple Methods for the Determination of the Dye Content of Fluorophore-Loaded Polymeric Particles. *Anal. Methods* **2012**, *4*, 1759–1768.
47. Patsenker, L. D.; Tatarets, A. L.; Povrozin, Y. A.; Terpetschnig, E. A. Long-Wavelength Fluorescence Lifetime Labels. *Bioanal. Rev.* **2011**, *3*, 115–137.
48. Berezin, M. Y.; Akers, W. J.; Guo, K.; Fischer, G. M.; Daltrozzo, E.; Zumbusch, A.; Achilefu, S. Long Fluorescence Lifetime Molecular Probes Based on Near Infrared Pyrrolopyrrole Cyanine Fluorophores for *in Vivo* Imaging. *Biophys. J.* **2009**, *97*, L22–L24.
49. Hoffmann, K.; Behnke, T.; Drescher, D.; Kneipp, J.; Resch-Genger, U. Lifetime-Based Discrimination between Spectrally Matching VIS and NIR Emitting Particle Labels and Probes. *Single Molecule Spectroscopy and Imaging IV. Proc. SPIE* **2011**, *7905*, 79051F-1–79051F-9.
50. Mathejczyk, J. E.; Pauli, J.; Dullin, C.; Napp, J.; Tietze, L. F.; Kessler, H.; Resch-Genger, U.; Alves, F. Spectroscopically Well-Characterized RGD Optical Probe as a Prerequisite for Lifetime-Gated Tumor Imaging. *Mol. Imaging* **2011**, *10*, 469–480.
51. *PicoQuant*, Application Note SymphoTime software; http://www.picoquant.de/technotes/appnote_spt_demo_workspace.pdf, 2008.
52. Posokhov, Y. O.; Ladokhin, A. S. Lifetime Fluorescence Method for Determining Membrane Topology of Proteins. *Anal. Biochem.* **2006**, *348*, 87–93.
53. Lunov, O.; Syrovets, T.; Loos, C.; Beil, J.; Delecher, M.; Tron, K.; Nienhaus, G. U.; Musyanovych, A.; Mailander, V.; Landfester; *et al*. Differential Uptake of Functionalized Polystyrene Nanoparticles by Human Macrophages and a Monocytic Cell Line. *ACS Nano* **2011**, *5*, 1657–1669.
54. Hillaireau, H.; Couvreur, P. Nanocarriers' Entry into the Cell: Relevance to Drug Delivery. *Cell. Mol. Life Sci.* **2009**, *66*, 2873–2896.
55. Clift, M. J. D.; Rothen-Rutishauser, B.; Brown, D. M.; Duffin, R.; Donaldson, K.; Proudfoot, L.; Guy, K.; Stone, V. The Impact of Different Nanoparticle Surface Chemistry and Size on Uptake and Toxicity in a Murine Macrophage Cell Line. *Toxicol. Appl. Pharmacol.* **2008**, *232*, 418–427.
56. Sun, D. X. Nanotheranostics: Integration of Imaging and Targeted Drug Delivery. *Mol. Pharmaceutics* **2010**, *7*, 1879–1879.
57. Liu, Y. X.; Li, W.; Lao, F.; Liu, Y.; Wang, L. M.; Bai, R.; Zhao, Y. L.; Chen, C. Y. Intracellular Dynamics of Cationic and Anionic Polystyrene Nanoparticles without Direct Interaction with Mitotic Spindle and Chromosomes. *Biomaterials* **2011**, *32*, 8291–8303.
58. Akers, W. J.; Berezin, M. Y.; Lee, H.; Achilefu, S. Predicting *in Vivo* Fluorescence Lifetime Behavior of Near-Infrared Fluorescent Contrast Agents Using *in Vitro* Measurements. *J. Biomed. Opt.* **2008**, *13*, 054042-1–054042-9.
59. Mathejczyk, J. E.; Pauli, J.; Dullin, C.; Resch-Genger, U.; Alves, F.; Napp, J. High-Sensitivity Detection of Breast Tumors *in Vivo* by Use of a pH-Sensitive Near-Infrared Fluorescence Probe. *J. Biomed. Opt.* **2012**, *17*, 076028-1–076028-10.
60. Rejman, J.; Oberle, V.; Zuhorn, I. S.; Hoekstra, D. Size-Dependent Internalization of Particles *via* the Pathways of Clathrin- and Caveolae-Mediated Endocytosis. *Biochem. J.* **2004**, *377*, 159–169.
61. dos Santos, T.; Varela, J.; Lynch, I.; Salvati, A.; Dawson, K. A. Quantitative Assessment of the Comparative Nanoparticle-Uptake Efficiency of a Range of Cell Lines. *Small* **2011**, *7*, 3341−3349.
62. Resch-Genger, U.; Pfeifer, D.; Monte, C.; Pilz, W.; Hoffmann, A.; Spieles, M.; Rurack, K.; Hollandt, J.; Taubert, D.; Schonenberger; *et al*. Traceability in Fluorometry: Part II. Spectral Fluorescence Standards. *J. Fluoresc.* **2005**, *15*, 315–336.
63. Kapusta P. *Sensitivity of FluoTime Series Lifetime Spectrometers*; PicoQuant GmbH Application Note, **2002**.
64. Krämer, B., Koberling, F., Tannert, A., Korte, T., Hermann A. *Fluorescence Lifetime Imaging (FLIM) Based Analysis of Lipid Organization in Hepatocytes Using the MicroTime 200*; PicoQuant GmbH Application Note, **2005**.